

# *Estimating tsunami inundation from hurricane storm surge predictions along the U.S. gulf coast*

**Alyssa Pampell-Manis, Juan Horrillo & Jens Figlus**

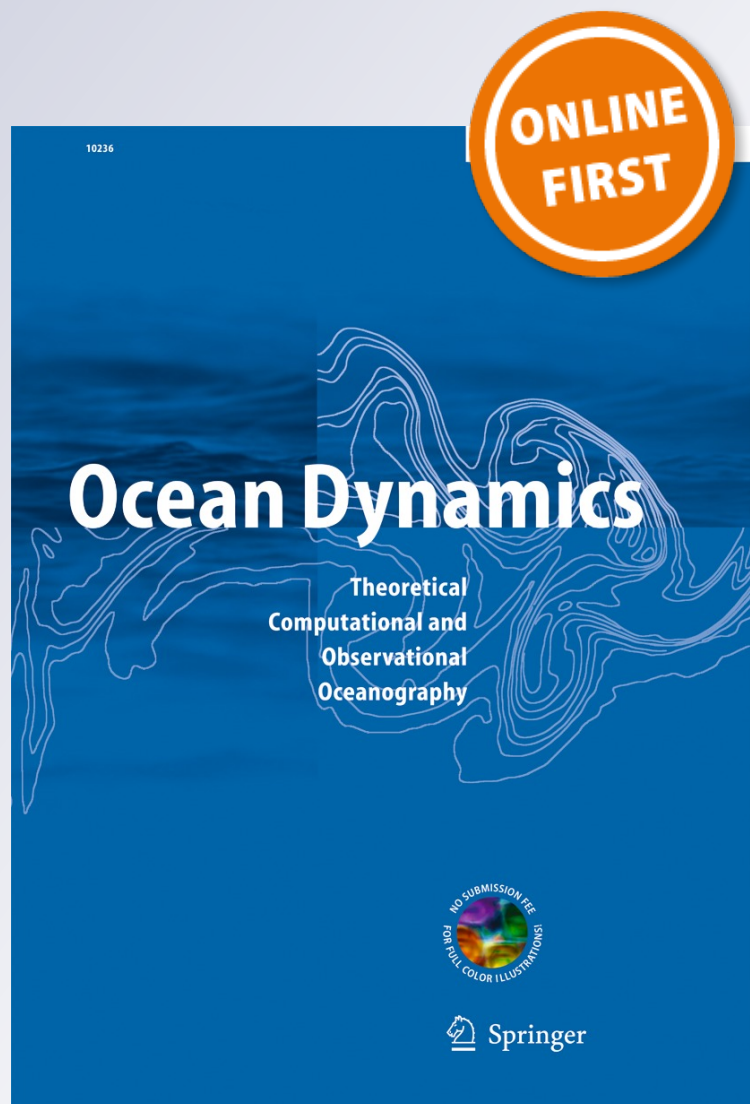
**Ocean Dynamics**

Theoretical, Computational and  
Observational Oceanography

ISSN 1616-7341

Ocean Dynamics

DOI 10.1007/s10236-016-0966-7



 Springer

**Your article is protected by copyright and all rights are held exclusively by Springer-Verlag Berlin Heidelberg. This e-offprint is for personal use only and shall not be self-archived in electronic repositories. If you wish to self-archive your article, please use the accepted manuscript version for posting on your own website. You may further deposit the accepted manuscript version in any repository, provided it is only made publicly available 12 months after official publication or later and provided acknowledgement is given to the original source of publication and a link is inserted to the published article on Springer's website. The link must be accompanied by the following text: "The final publication is available at [link.springer.com](http://link.springer.com)".**

# Estimating tsunami inundation from hurricane storm surge predictions along the U.S. Gulf Coast

Alyssa Pampell-Manis<sup>1,2</sup>  · Juan Horrillo<sup>1</sup> · Jens Figlus<sup>1</sup>

Received: 1 March 2016 / Accepted: 10 June 2016  
© Springer-Verlag Berlin Heidelberg 2016

**Abstract** Gulf of Mexico (GOM) coasts have been included in the U.S. Tsunami Warning System since 2005. While the tsunami risk for the GOM is low, tsunamis generated by local submarine landslides pose the greatest potential threat, as evidenced by several large ancient submarine mass failures identified in the northern GOM basin. Given the lack of significant historical tsunami evidence in the GOM, the potential threat of landslide tsunamis in this region is assessed from a worst-case scenario perspective based on a set of events including the large ancient failures and most likely extreme events determined by a probabilistic approach. Since tsunamis are not well-understood along the Gulf Coast, we investigate tsunami inundation referenced to category-specific hurricane storm surge levels, which are relatively well established along the Gulf Coast, in order to provide information for assessing the potential threat of tsunamis which is more understandable and accessible to emergency managers. Based on tsunami inundation studies prepared for the communities of South Padre Island, TX, Galveston, TX, Mobile, AL, Panama City, FL, and Tampa, FL, we identify regional trends of tsunami inundation in terms of modeled storm surge inundation.

The general trends indicate that tsunami inundation can well exceed the level of storm surge from major hurricanes in open beachfront and barrier island regions, while more interior areas are less threatened. Such information can be used to better prepare for tsunami events as well as provide a preliminary estimate of tsunami hazard in locations where detailed tsunami inundation studies have not been completed.

**Keywords** Tsunami · Inundation mapping · Flood risk · Hazard evaluation · Gulf of Mexico

## 1 Introduction

The U.S. Tsunami Warning System has included Gulf of Mexico (GOM) coasts since 2005 in order to enable local emergency management to act in response to tsunami warnings. To plan for the warning response, emergency managers must understand what specific areas within their jurisdictions are threatened by tsunamis. Coastal hazard areas susceptible to tsunami inundation can be determined by historical events, by modeling potential tsunami events (worst-case scenarios), or by using a probabilistic approach to determine the rate of recurrence or likelihood of exceeding a certain threshold. As the GOM coastal regions have no significant recent historical tsunami records, numerical modeling and probabilistic methodologies for source identification must be used to determine coastal hazard zones.

Potential tsunami sources for the GOM are local submarine landslides (ten Brink et al. 2009b); sources outside the GOM are considered a very low threat and may not significantly impact GOM coastal communities or infrastructure (Knight 2006). Although a massive tsunamigenic

---

This article is part of the Topical Collection on the *14th International Workshop on Wave Hindcasting and Forecasting in Key West, Florida, USA, November 8–13, 2015*

---

Responsible Editor: Diana Greenslade

---

✉ Alyssa Pampell-Manis  
alyssa.p.manis@nasa.gov

<sup>1</sup> Department of Ocean Engineering, Texas A&M University at Galveston, Galveston, TX, 77553, USA

<sup>2</sup> Present address: HX5 LLC, Houston, TX, 77058, USA

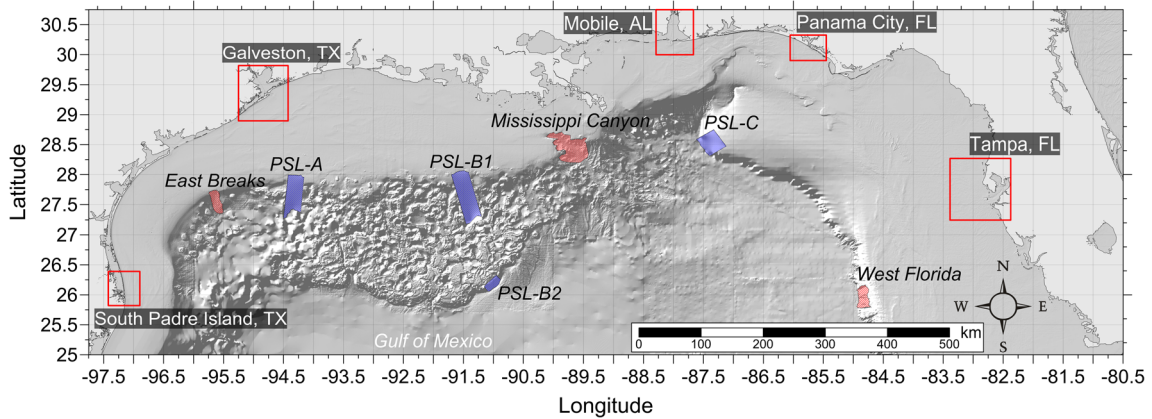


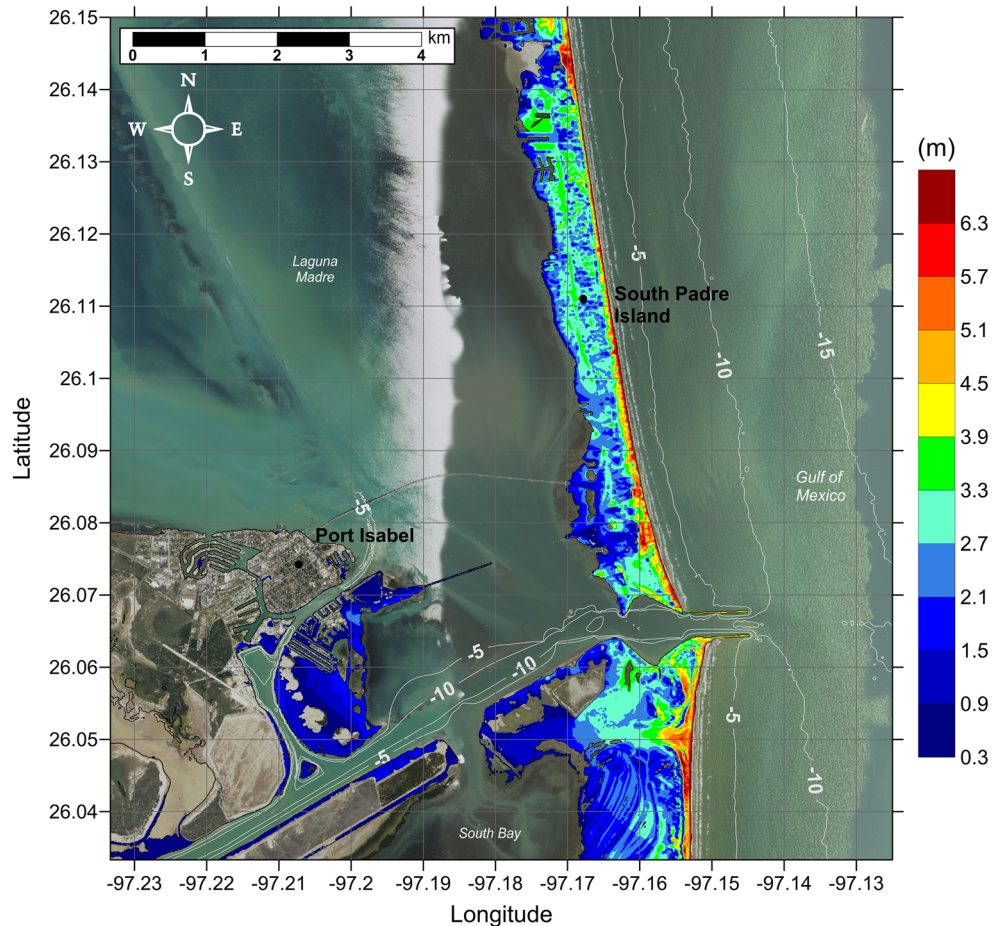
**Fig. 1** Northern Gulf of Mexico domain used in NEOWAVE to model wave propagation. Footprints of submarine landslides are shown as colored hatched regions: *red regions* correspond to identified historical failures; *blue regions* correspond to created probabilistic landslides.

*Red rectangles* indicate 3 arcsecond ( $\sim 90$  m) domains of each coastal community where tsunami inundation is modeled. The *contour* drawn is the zero-meter contour for land elevation

underwater landslide in the GOM is considered a potential hazard, the frequency of such events (though not well constrained) is probably quite low based on historical evidence (Dunbar and Weaver 2008) and available data on ages of failures which suggest they were probably active prior

to 7000 years ago when large quantities of sediments were emptied into the GOM (ten Brink et al. 2009b). However, sediments continue to empty into the GOM, mainly from the Mississippi River, contributing to slope steepening and the increase of fluid pore pressure in sediments which may

**Fig. 2** Maximum of maximums tsunami inundation depth (in meters) in South Padre Island, TX, calculated as the maximum inundation depth in each grid cell from an ensemble of all tsunami sources considered. The contours drawn and labeled are at  $-5$ ,  $-10$ , and  $-15$  m levels



lead to unstable slopes that can be subsequently triggered to failure by seismic loading (Masson et al. 2006; ten Brink et al. 2009a; Dugan and Stigall 2010; Harbitz et al. 2014). In addition, the GOM basin features an almost completely enclosed body of water with a curved coastline that makes even unlikely tsunami events originating inside this confined space potentially hazardous to the entire Gulf Coast. Waves tend to refract along continental slopes; thus, given the curved geomorphology of the GOM shelf and the concave shape of the coastline, any outgoing tsunami wave could potentially affect the opposite coast in addition to the coast close to the landslide source.

Three large-scale historical (ancient) submarine landslides with tsunamigenic potential have been identified within the GOM (ten Brink et al. 2009b), representing possible worst-case tsunami scenarios affecting GOM coasts in the past. In order to generate a more complete picture of landslide tsunami potential in the GOM, a probabilistic approach has been implemented to develop four additional synthetic landslide sources which fill gaps along the continental shelf between the historical landslide sources (Pampell-Manis et al. 2016). These probabilistic tsunami sources are considered to be the maximum credible events

that could happen in a particular region of the GOM according to the local bathymetry, seafloor slope, sediment information, and seismic loading. The probabilistic maximum credible events together with the historical sources form a suite of tsunami sources that have been used within coupled 3D and 2D numerical models to model tsunami generation and propagation throughout the GOM and to develop high-resolution inundation maps for the inundation-prone areas of five selected communities along the Gulf Coast: South Padre Island, TX; Galveston, TX; Mobile, AL; Panama City, FL; and Tampa, FL (Horrillo et al. 2015). These inundation studies showed that tsunamis triggered by massive submarine landslides have the potential to cause widespread and significant inundation of coastal cities.

While high-resolution tsunami inundation studies have been completed for these five communities and are planned for additional locations, vulnerability assessments are still essential for coastal locations where inundation studies have not yet been performed or planned or where there is a lack of high-resolution bathymetric and/or elevation data. Therefore, we aim to extend the results of the completed mapping studies in order to provide estimates of tsunami inundation zones for hazard mitigation efforts in

**Fig. 3** Hurricane category which produces inundation at high tide that best matches the MOM tsunami inundation shown in Fig. 2 for South Padre Island, TX. The contours drawn and labeled are at  $-5$ ,  $-10$ , and  $-15$  m levels

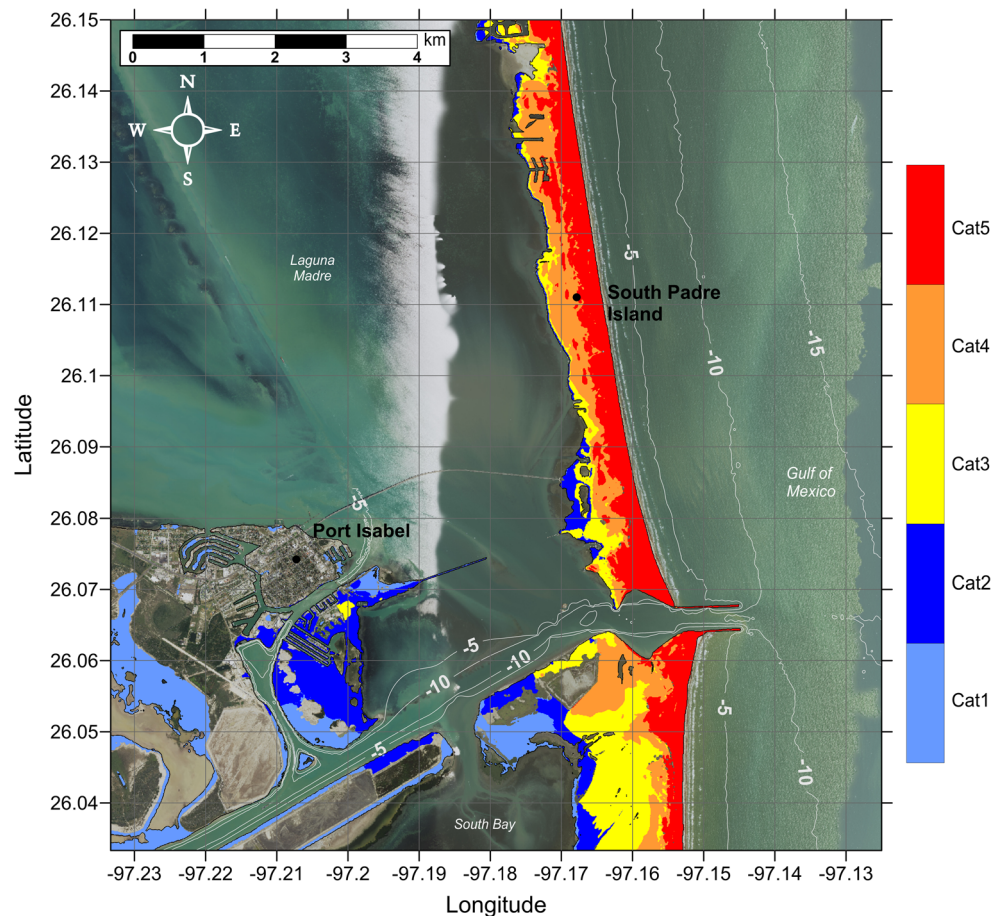
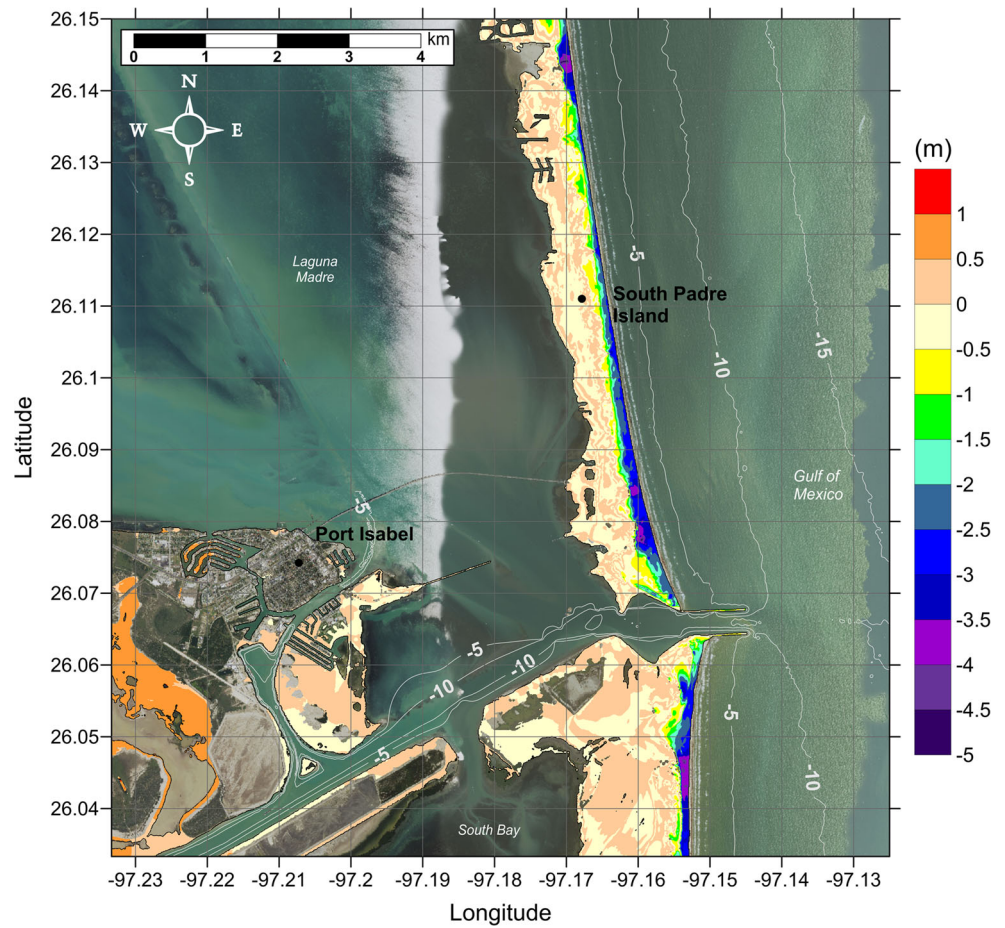


**Fig. 4** Actual difference  $\Delta\zeta$  (in meters) between SLOSH MOM storm surge inundation and MOM tsunami inundation for the best-match hurricane category shown in Fig. 3 for South Padre Island, TX. Note that negative values indicate where tsunami inundation is higher than hurricane inundation, and *pale colors* indicate relatively good agreement between tsunami and storm surge inundation, i.e.,  $|\Delta\zeta| \leq 0.5$  m. The *contours* drawn and labeled are at  $-5$ ,  $-10$ , and  $-15$  m levels



un-mapped locations. Inundation maps with even low resolution are useful to emergency managers to create first-order evacuation maps, and some methods currently exist

to provide low-resolution estimates of hazard zones for regions which do not currently have or warrant high-resolution maps. For example, guidance given by the

**Fig. 5** Maximum of maximums tsunami inundation depth (in meters) in Galveston, TX, calculated as the maximum inundation depth in each grid cell from an ensemble of all tsunami sources considered. The *dashed black line* indicates the location of the seawall. The *contours* drawn and labeled are at  $-5$ ,  $-10$ , and  $-15$  m levels

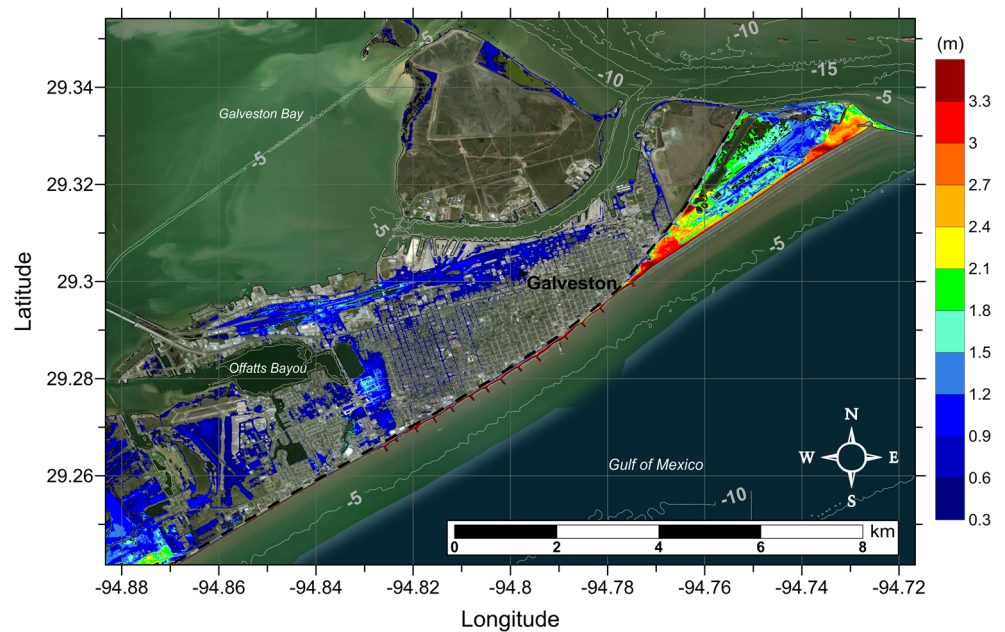
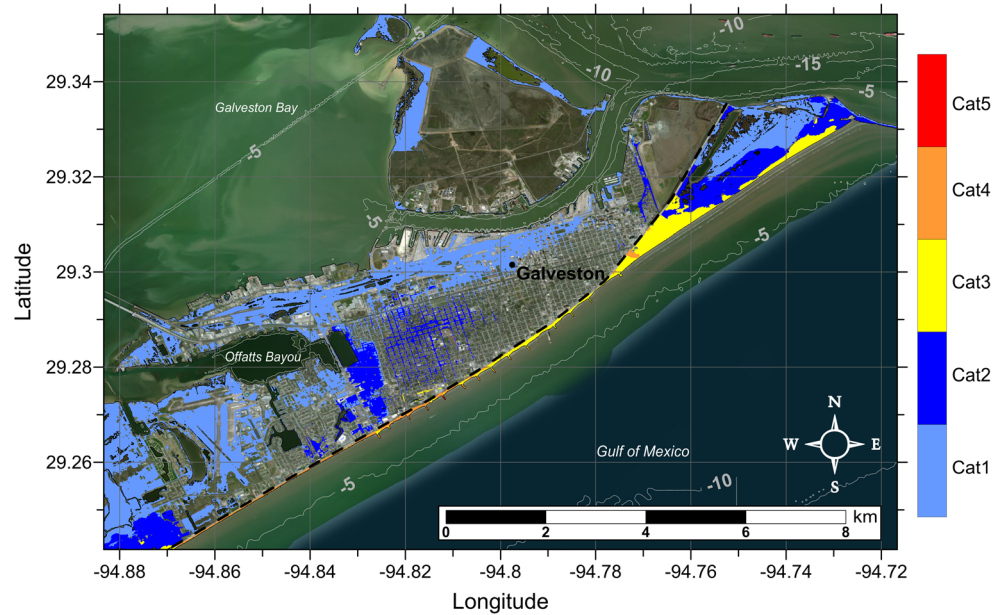


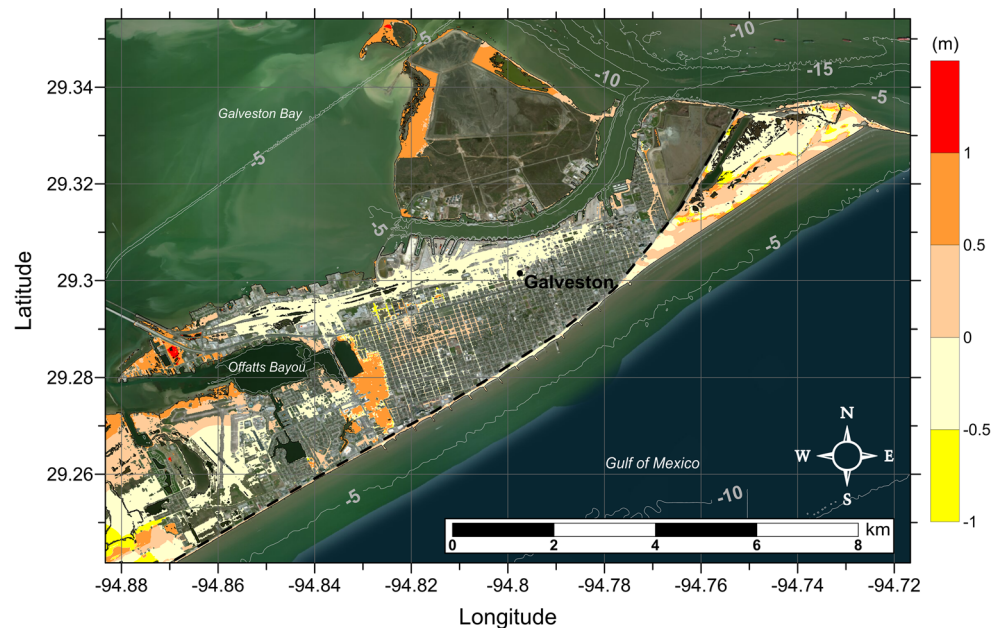
**Fig. 6** Hurricane category which produces inundation at high tide that best matches the MOM tsunami inundation shown in Fig. 5 for Galveston, TX. The dashed black line indicates the location of the seawall. The contours drawn and labeled are at  $-5$ ,  $-10$ , and  $-15$  m levels



National Tsunami Hazard Mitigation Program (NTHMP) Mapping and Modeling Subcommittee in “Guidelines and Best Practices to Establish Areas of Tsunami Inundation for Non-modeled or Low-hazard Regions” (available from <http://nws.weather.gov/nthmp/documents/Inundationareguidelinesforlowhazardareas.pdf>) recommends that coastal areas and areas along ocean-connected waterways that are below 10 m (33 ft) elevation are at risk for most tsunamis, and rare and larger tsunamis may inundate above this elevation. However, in low-lying coastal regions such as along the Gulf Coast, the 10-m (33 ft) elevation

contour is too far inland to be reasonably applicable for estimating potential tsunami inundation zones. The guidance additionally suggests that low-lying areas are prone to inundation within 3 km (1.9 mi) inland for locally generated tsunamis and within 2 km (1.3 mi) inland for distant sources. While these distances may be reasonable for some regions of the Gulf Coast, prevalent bathymetric and topographic features such as barrier islands/peninsulas complicate the method of delineating inundation-prone areas based on distance from the shoreline. As a result, the purpose of the current work is to develop a methodology which compares

**Fig. 7** Actual difference  $\Delta\zeta$  (in meters) between SLOSH MOM storm surge inundation and MOM tsunami inundation for the best-match hurricane category shown in Fig. 6 for Galveston, TX. Note that negative values indicate where tsunami inundation is higher than hurricane inundation, and pale colors indicate relatively good agreement between tsunami and storm surge inundation, i.e.,  $|\Delta\zeta| \leq 0.5$  m. The dashed black line indicates the location of the seawall. The contours drawn and labeled are at  $-5$ ,  $-10$ , and  $-15$  m levels



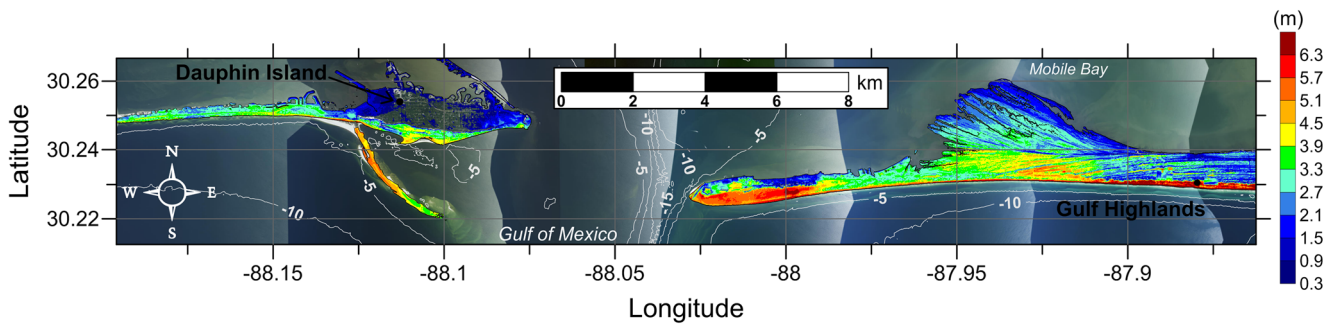


**Fig. 8** Maximum of maximums tsunami inundation depth (in meters) in Dauphin Island/Gulf Highlands, AL, calculated as the maximum inundation depth in each grid cell from an ensemble of all tsunami sources considered. The contours drawn and labeled are at  $-5$ ,  $-10$ , and  $-15$  m levels

modeled tsunami inundation to modeled/predicted hurricane storm surge. Specifically, we aim to identify the hurricane category which produces modeled maximum storm surge that best approximates the maximum tsunami inundation modeled in Horrillo et al. (2015). Even though many physical aspects of storm surge inundation are completely different from those of tsunamis (time scale, triggering mechanism, inundation process, etc.), good agreement or clear trends between tsunami and storm surge flooding on a regional scale can be used to provide first-order estimates of potential tsunami inundation in communities where detailed inundation maps have not yet been developed or are not possible due to unavailability of high-resolution bathymetry/elevation data. Additionally, since tsunamis are not well understood as a threat along the Gulf Coast, but hurricane hazards are well known, this method of referencing anticipated tsunami inundation to storm surge provides a way for GOM emergency managers to better prepare for potential tsunami events based on more understandable and accessible information.

Although the probability of a large-scale tsunami event in the GOM is low, this study has indicated that tsunami events with characteristics similar to those detailed in Horrillo et al. (2015) have the potential to cause severe flooding and damage to GOM coastal communities that is similar to or even greater than that seen from major hurricanes, particularly in open beach and barrier island regions. The results of this

work are intended to provide guidance to local emergency managers to help with managing urban growth, evacuation planning, and public education with the vision to mitigate potential GOM tsunami hazards.

This paper is organized as follows. Section 2 briefly describes the tsunami sources used for tsunami modeling Section 2.1 and the numerical models themselves Section 2.2. The comparison of tsunami inundation with hurricane storm surge inundation is given in Section 3 for the five selected Gulf Coast communities. Concluding remarks on the general trends seen among the communities and implications for other regions are given in Section 4.

## 2 Tsunami inundation modeling

### 2.1 Landslide tsunami sources

Seven large-scale landslide configurations were created assuming an unstable (gravity-driven) sediment deposit condition. Three of these landslide configurations are historical events identified by ten Brink et al. (2009b): the East Breaks, Mississippi Canyon, and West Florida submarine landslides, which are shown as red hatched regions in Fig. 1. The other four were obtained using a probabilistic methodology based on work by Marezki et al. (2007) and Grilli et al. (2009) and extended for the GOM

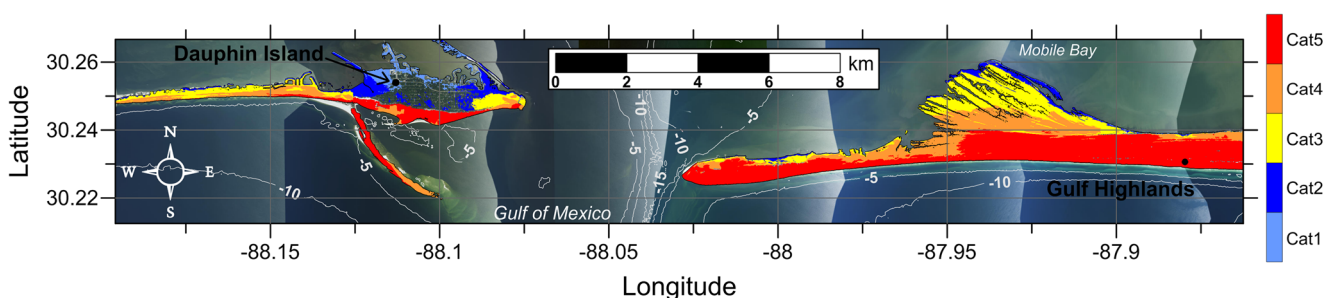


**Fig. 9** Hurricane category which produces inundation at high tide that best matches the MOM tsunami inundation shown in Fig. 8 for Dauphin Island/Gulf Highlands, AL. The contours drawn and labeled are at  $-5$ ,  $-10$ , and  $-15$  m levels

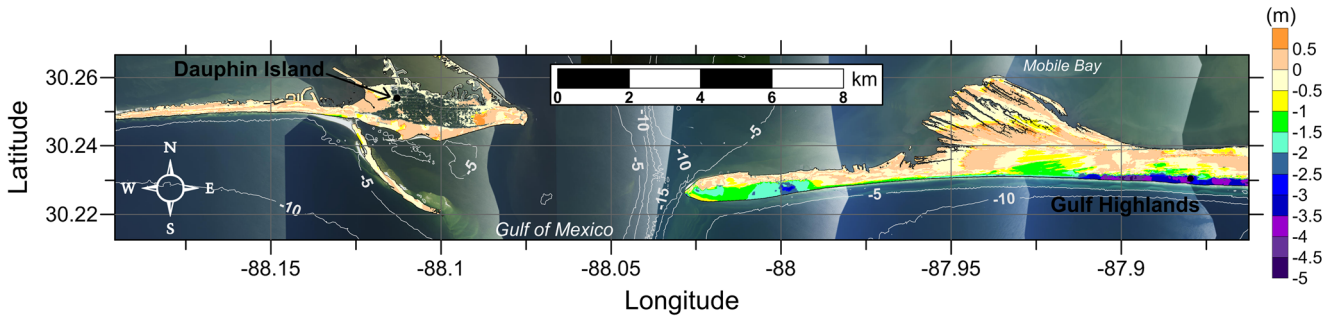


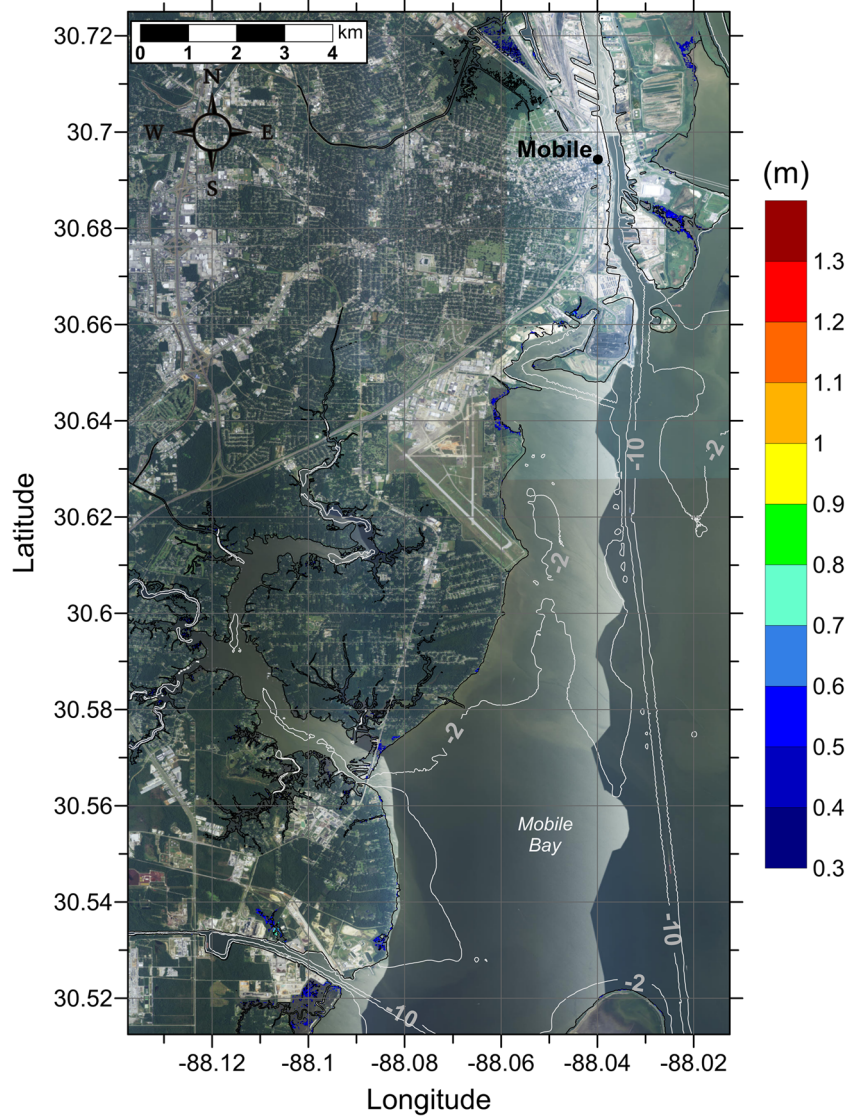
**Fig. 10** Actual difference  $\Delta\zeta$  (in meters) between SLOSH MOM storm surge inundation and MOM tsunami inundation for the best-match hurricane category shown in Fig. 9 for Dauphin Island/Gulf Highlands, AL. Note that negative values indicate where tsunami

inundation is higher than hurricane inundation, and *pale colors* indicate relatively good agreement between tsunami and storm surge inundation, i.e.,  $|\Delta\zeta| \leq 0.5$  m. The *contours* drawn and labeled are at  $-5$ ,  $-10$ , and  $-15$  m levels

by Pampell-Manis et al. (2016). The probabilistic landslide configurations were determined based on distributions

of previous GOM submarine landslide dimensions through a Monte Carlo Simulation (MCS) approach. The MCS

**Fig. 11** Maximum of maximums tsunami inundation depth (in meters) in Mobile, AL, calculated as the maximum inundation depth in each grid cell from an ensemble of all tsunami sources considered. The *contours* drawn and labeled are at  $-2$  and  $-10$  m levels



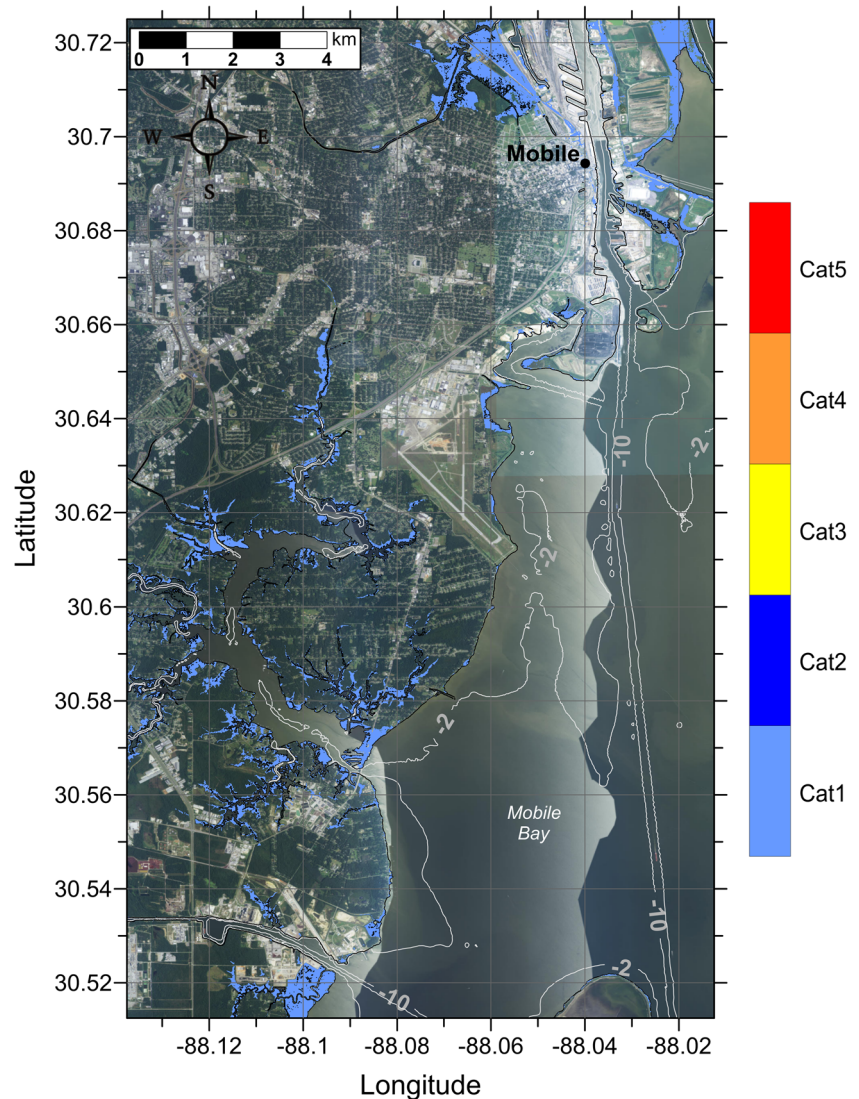
methodology incorporates a statistical correlation method for capturing trends seen in observational data for landslide size parameters while still allowing for randomness in the generated landslide dimensions. Slope stability analyses are performed for the MCS-generated trial landslide configurations using landslide and sediment properties and regional seismic loading (Peak Horizontal ground Acceleration, PHA) to determine landslide configurations which fail and produce a tsunami. The probability of each tsunami-genic failure is calculated based on the joint probability of the earthquake PHA and the probability that the trial landslide fails and produces a tsunami wave above a certain threshold. Those failures which produce the largest tsunami amplitude and have the highest probability of occurrence are deemed the most extreme probabilistic events, and the dimensions of these events are averaged to determine maximum credible probabilistic sources. The four maximum credible Probabilistic Submarine Landslides (PSLs) used as

tsunami sources for this study are termed PSL-A, PSL-B1, PSL-B2, and PSL-C and are shown as blue hatched regions in Fig. 1. A complete discussion of the submarine landslide sources used here is given in Horrillo et al. (2015) and Pampell-Manis et al. (2016). Specific details on the size parameters of each landslide source are given in Tables 7-20 of Horrillo et al. (2015).

## 2.2 Numerical models

For the seven landslide tsunami sources considered here, tsunami wave development and subsequent propagation and inundation of coastal communities was modeled using coupled 3D and 2D numerical models (Horrillo et al. 2015). The tsunami generation phase was modeled using the 3D model TSUNAMI3D (Horrillo 2006; Horrillo et al. 2013), which solves the finite difference approximation of the full Navier-Stokes equations and the incompressibility (continuity)

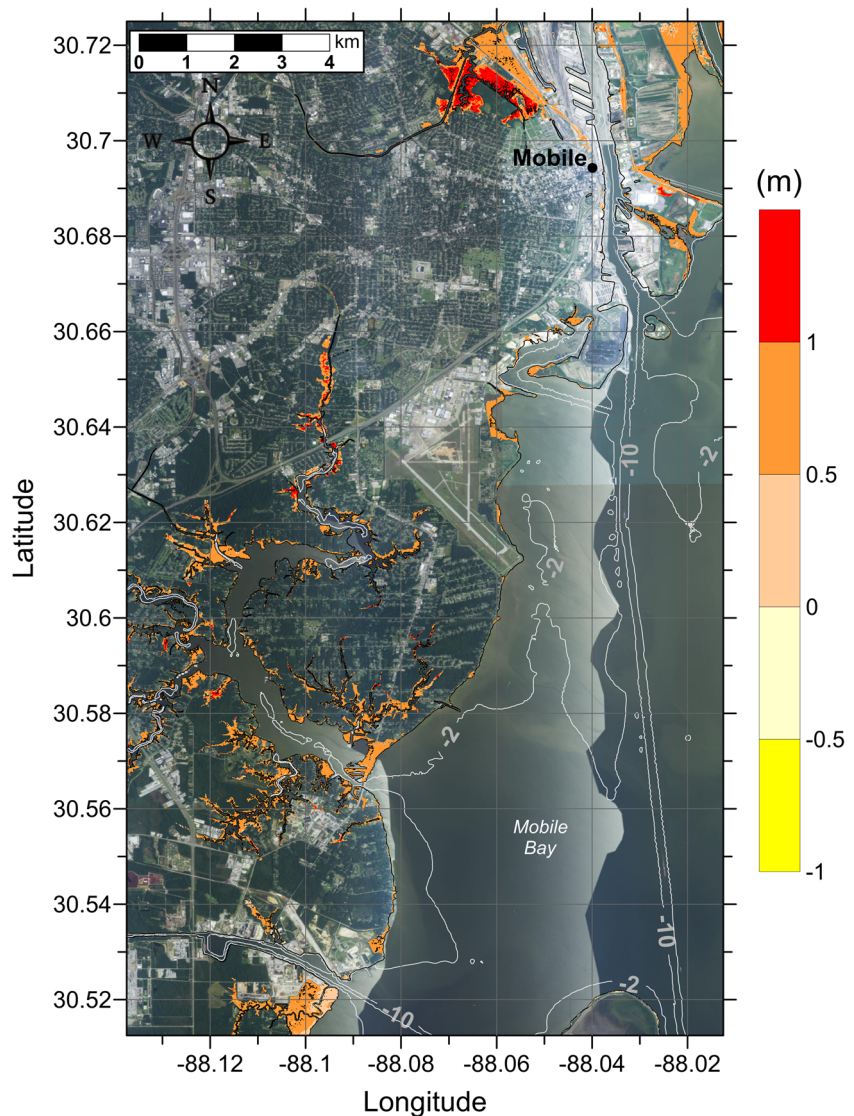
**Fig. 12** Hurricane category which produces inundation at high tide that best matches the MOM tsunami inundation shown in Fig. 11 for Mobile, AL. The contours drawn and labeled are at  $-2$  and  $-10$  m levels



equation. Water and landslide material are represented as Newtonian fluids with different densities, and the landslide-water and water-air interfaces are tracked using the volume of fluid (VOF) method of Hirt and Nichols (1981), which is simplified to account for the large horizontal/vertical aspect ratio of the tsunami wave and the selected computational cell size required to construct an efficient 3D grid. The pressure term is split into hydrostatic and non-hydrostatic components. Although TSUNAMI3D has the capability of variable grids, the nesting capability necessary for modeling detailed inundation of coastal regions is too computationally intensive within the fully 3D model; thus, detailed inundation modeling is achieved by coupling the 3D model to a 2D model. Once the tsunami wave generated by the 3D model is fully developed, the wave is passed as an initial condition to the 2D model for modeling wave propagation and coastal inundation. The generated wave is considered

fully developed when the total wave energy (potential plus kinetic) reaches a maximum and before the wave leaves the computational domain, as discussed in López-Venegas et al. (2015). The 2D model used here is NEOWAVE (Yamazaki et al. 2008), a depth-integrated and nonhydrostatic model built on the nonlinear shallow water equations which includes a momentum-conserved advection scheme to model wave breaking and two-way nested grids for modeling higher-resolution wave runup and inundation. Propagation and inundation are calculated via a series of nested grids of increasing resolution, from 15 arcsecond (450 m) resolution for a domain encompassing the entire northern GOM (Fig. 1), to finer resolutions of 3 arcseconds (90 m, from NOAA NCEI Coastal Relief Models), 1 arcsecond (30 m), and 1/3 arcsecond (10 m, from NOAA NCEI Tsunami Inundation Digital Elevation Models [DEMs]) to model detailed inundation of the most populated/inundation-prone

**Fig. 13** Actual difference  $\Delta\zeta$  (in meters) between SLOSH MOM storm surge inundation and MOM tsunami inundation for the best-match hurricane category shown in Fig. 12 for Mobile, AL. Note that negative values indicate where tsunami inundation is higher than hurricane inundation, and *pale colors* indicate relatively good agreement between tsunami and storm surge inundation, i.e.,  $|\Delta\zeta| \leq 0.5$  m. The *contours* drawn and labeled are at  $-2$  and  $-10$  m levels



areas of each coastal community. The 3-arcsecond (90 m) grids encompassing each coastal community studied here are shown by red rectangles in Fig. 1.

### 3 Tsunami and hurricane storm surge inundation

Tsunami inundation depth and extent has been modeled for five selected coastal communities: South Padre Island, TX; Galveston, TX; Mobile, AL; Panama City, FL; and Tampa, FL (Horrillo et al. 2015). Inundation (flooding) is determined by subtracting land elevation from water elevation, and elevations used are in reference to the mean high water (MHW) tidal datum. For this study, the tsunami inundation depth/extent modeled for each community is the maximum-of-maximums (MOM) inundation, which is calculated as the maximum inundation depth from an ensemble of inundation depths produced by each of the seven tsunami sources considered. That is, once inundation in a community has been modeled for each of the seven sources, the overall maximum inundation depth in each computational grid cell is taken as the MOM tsunami inundation in that cell. This approach gives a worst-case scenario perspective of estimated tsunami inundation for each coastal community. It is worth noting, however, that for the communities along the northern and eastern GOM (Mobile, AL, Panama City, FL,

and Tampa, FL), the MOM tsunami inundation is produced solely by the Mississippi Canyon failure. That historical failure is the largest in both area and volume of material removed and therefore produces the highest amplitude wave of all sources simulated. MOM tsunami inundation in South Padre Island, TX, and Galveston, TX, is also dominated by this source, though in some isolated stretches, the MOM inundation comes from other sources as well: East Breaks and PSL-A in South Padre Island (the sources closest to that location), and PSL-A and PSL-C in Galveston. See Horrillo et al. (2015) for details of the inundation modeling and figures of the maximum tsunami amplitude produced by each landslide (their Figs.12, 16, 20, 24, 28, 32, and 36) which show the overall dominance of the Mississippi Canyon source.

Due to the limitations on availability of high-resolution (1/3 arcsecond) DEMs, detailed inundation maps for all communities along the Gulf Coast are not yet possible. In an effort to develop a first-order estimate of potential tsunami inundation for those locations where detailed inundation maps have not yet been developed, we compare tsunami inundation modeled for the communities mentioned above to hurricane storm surge modeled data. The motivation for and implications of this approach are twofold. It provides a way to assess tsunami inundation in un-mapped communities based on existing storm surge flood data and also

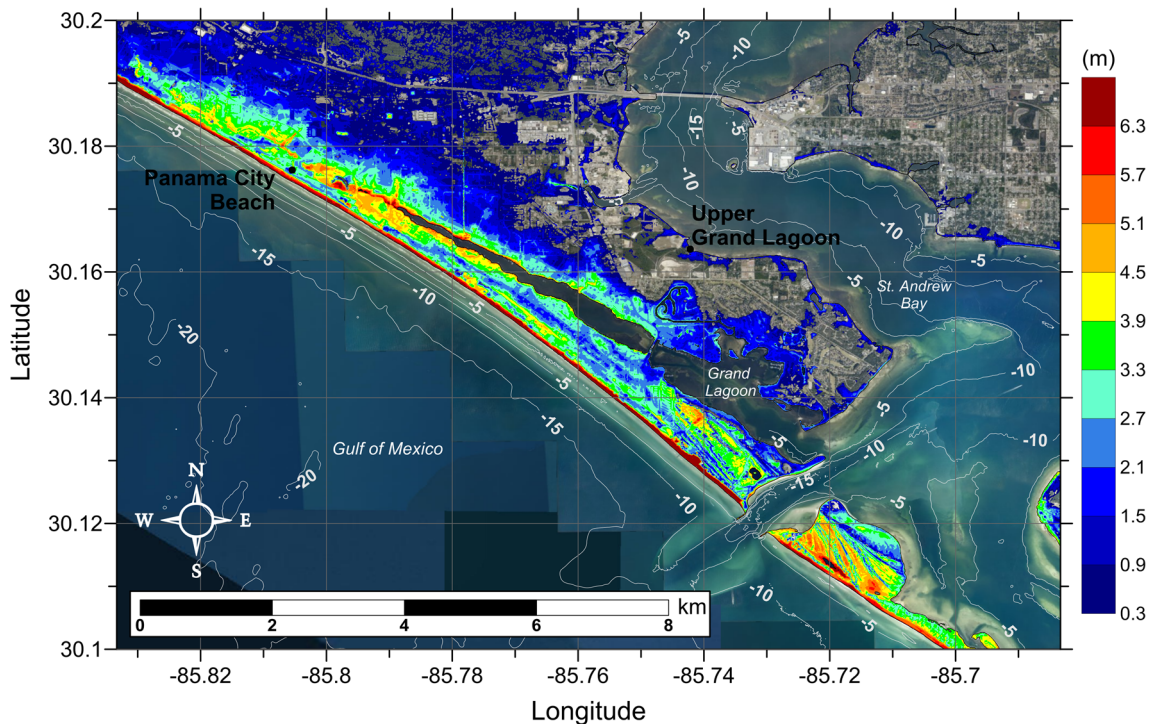


**Fig. 14** Maximum of maximums tsunami inundation depth (in meters) in the Panama City Beach, FL region, calculated as the maximum inundation depth in each grid cell from an ensemble of all tsunami sources considered. The contours drawn and labeled are at  $-5$ ,  $-10$ ,  $-15$ , and  $-20$  m levels

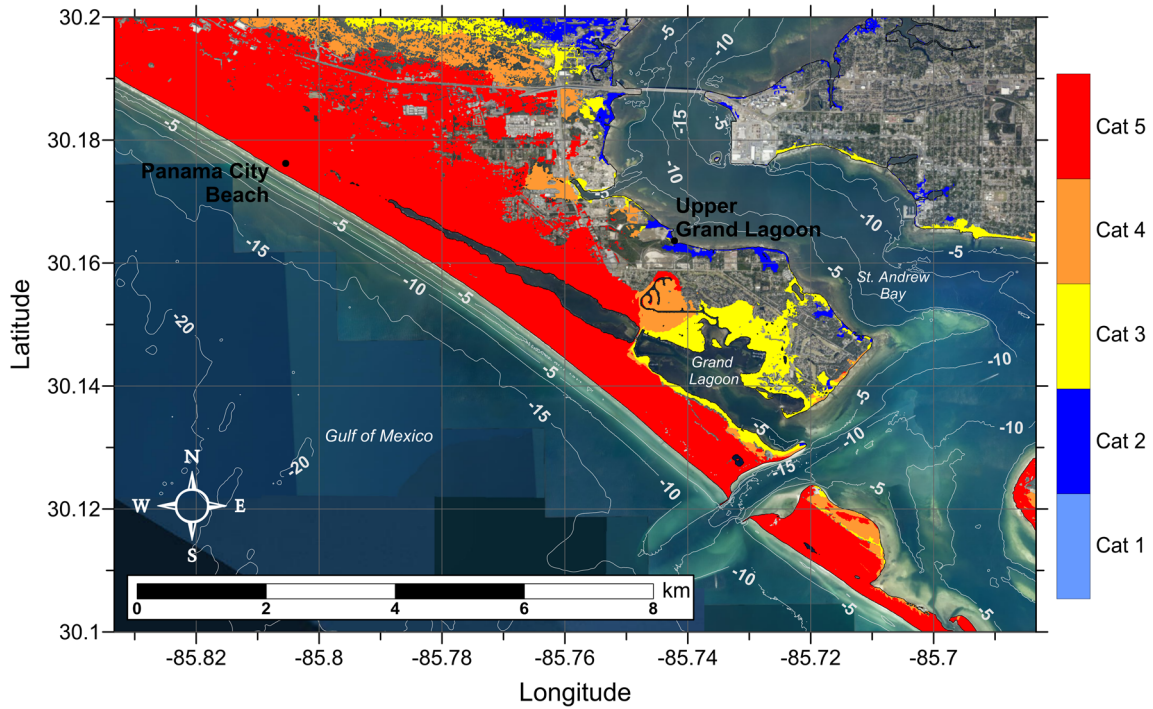


**Fig. 15** Hurricane category which produces inundation at high tide that best matches the MOM tsunami inundation shown in Fig. 14 for the Panama City Beach, FL region. The contours drawn and labeled are at  $-5$ ,  $-10$ ,  $-15$ , and  $-20$  m levels

relates the level of tsunami hazard to that of another hazard that is better defined in this region. Tsunamis are not

well understood as a threat along the Gulf Coast, making tsunami hazard mitigation efforts somewhat difficult.

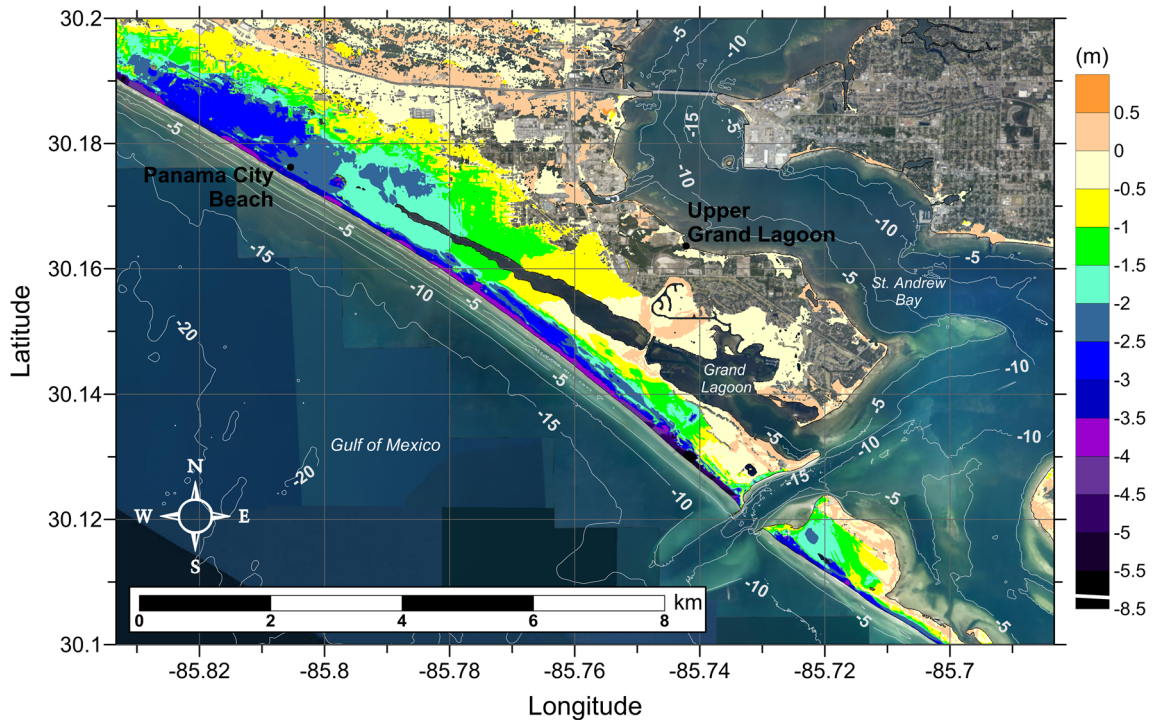


**Fig. 16** Actual difference  $\Delta\zeta$  (in meters) between SLOSH MOM storm surge inundation and MOM tsunami inundation for the best-match hurricane category shown in Fig. 15 for the Panama City Beach, FL region. Note that negative values indicate where tsunami

inundation is higher than hurricane inundation, and pale colors indicate relatively good agreement between tsunami and storm surge inundation, i.e.,  $|\Delta\zeta| \leq 0.5$  m. The contours drawn and labeled are at  $-5$ ,  $-10$ ,  $-15$ , and  $-20$  m levels

However, hurricanes are a relatively well-understood threat in this region, and hurricane preparedness approaches are well developed. As a result, comparisons of tsunami and hurricane storm surge inundation levels provide a more understandable and accessible idea of the level of hazard presented by potential tsunami events and can serve as a basis for tsunami preparedness efforts.

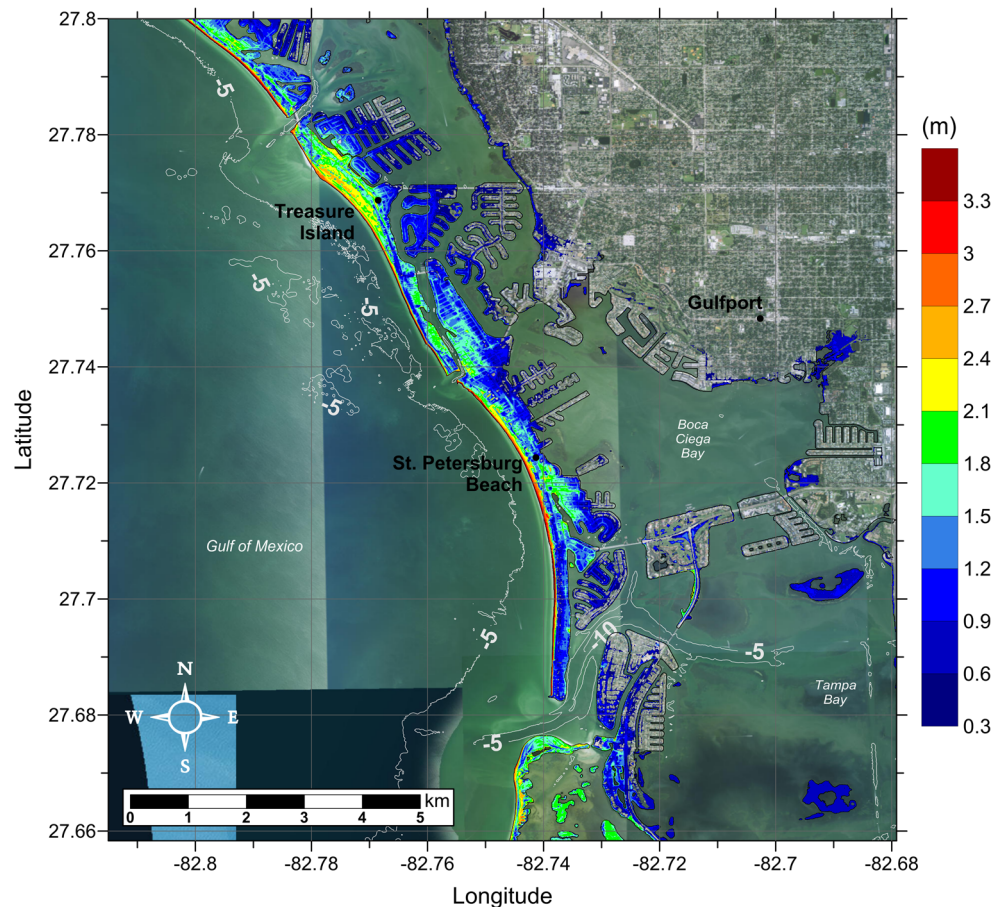
The hurricane storm surge data used here is that available from the Sea, Lake, and Overland Surges from Hurricanes (SLOSH) model (<http://www.nhc.noaa.gov/surge/slosh.php>). The SLOSH model was developed by the National Weather Service (NWS) to provide estimates of storm surge heights caused by historical, predicted, or hypothetical hurricanes based on different values for atmospheric pressure, hurricane size, forward speed, and track. It uses a polar, elliptical, or hyperbolic grid for computations, leading to higher resolutions near coastal areas of interest. Some limitations of the SLOSH model should be acknowledged. Resolution of the model varies from tens of meters to a kilometer or more. Near the coastal communities of interest here, resolution is on the order of 1 km (0.6 mi). Sub-grid scale water and topographic features such as channels, rivers, levees, and roads, are parameterized instead of being explicitly modeled. Despite these limitations, the hurricane

storm surge data from the SLOSH model is currently the best data publicly available for our purposes, and efforts have been made to ensure the validity of the SLOSH data in performing comparisons with tsunami inundation.

The SLOSH MOM results provide the worst-case storm surge for a given hurricane category and initial tide level based on a set of model runs with various combinations of parameters such as forward speed, trajectory, and landfall location. To perform the storm surge and tsunami comparisons, SLOSH storm surge elevation data was first converted to meters and adjusted from the NAVD88 to the MHW vertical datum using NOAA's VDatum tool (<http://vdatum.noaa.gov/>). Due to the relatively low resolution of the SLOSH data as compared to the DEMs used for tsunami modeling, the SLOSH data was interpolated to 1/3 arcsecond (10 m) resolution using a kriging method. Inundation was then determined by subtracting land elevation from the storm surge elevation.

Here, an initial high tide level is used for the SLOSH MOM results in order to compare the worst-case tsunami inundation with a worst-case storm surge scenario. The high tide SLOSH MOM data includes effects of the highest predicted tide level at each location. In comparison, water elevations in the tsunami modeling are based on the

**Fig. 17** Maximum of maximums tsunami inundation depth (in meters) in the southern greater Tampa-St. Petersburg-Clearwater area, calculated as the maximum inundation depth in each grid cell from an ensemble of all tsunami sources considered. The contours drawn and labeled are at  $-5$  and  $-10$  m levels



MHW datum, which averages the high water levels over the National Tidal Datum Epoch (NTDE). Within the GOM, tidal ranges are relatively small, with diurnal ranges on the order of 1.5 ft (0.5 m) for most of the communities studied here and slightly higher at around 2.5 ft (0.8 m) for the Tampa, FL area. Thus, differences between highest tide levels and the mean of the highest tide levels are expected to be relatively small, though local bathymetric effects combined with tidal effects can still be significant.

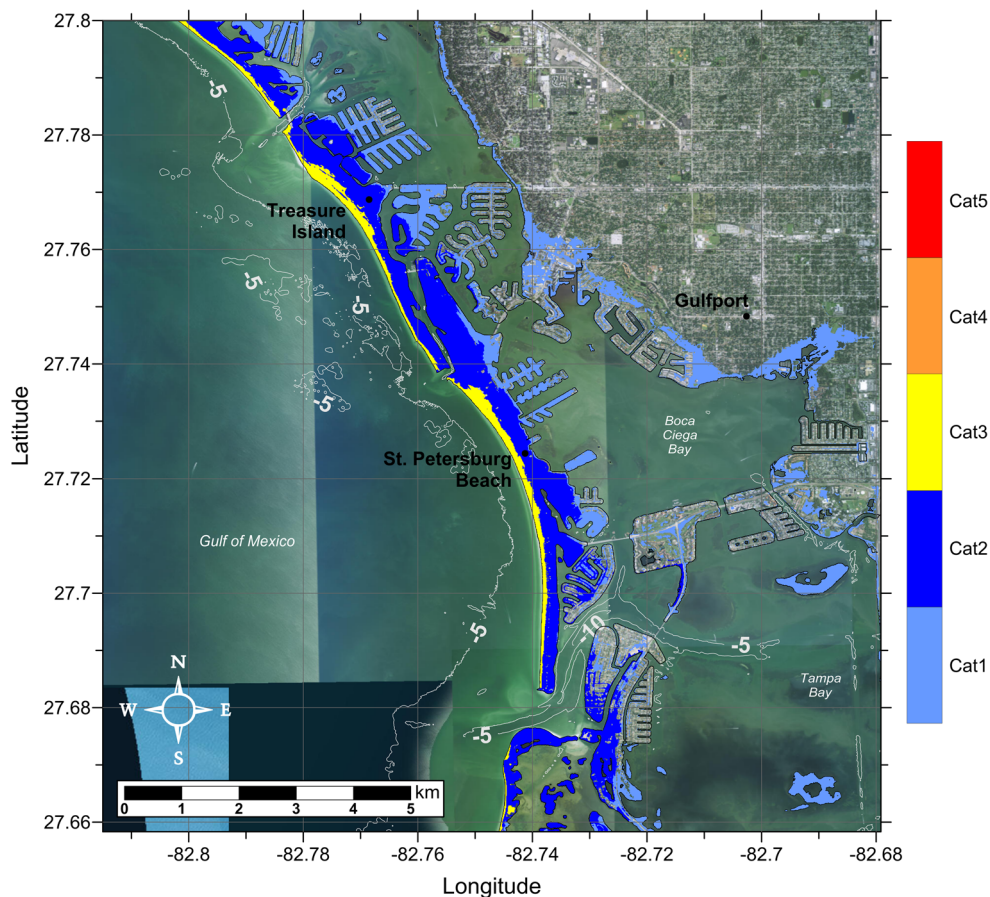
It should be noted that the updated Saffir-Simpson Hurricane Wind Scale which delineates hurricane categories 1–5 does not include storm surge as a component of the measure of hurricane intensity and that other methods may capture the physics of hurricane severity and damage in a more appropriate manner (e.g., Kantha 2006; Basco and Klentzman 2006; Irish and Resio 2010). However, the SLOSH MOM results take into account thousands of scenarios for a given hurricane category, resulting in a composite worst-case storm surge scenario for each Saffir-Simpson hurricane category. Thus, since hurricane preparedness, storm surge evacuation zones, and hazard mitigation efforts are based on hurricane category assignment, we aim to determine the hurricane category which produces MOM storm surge inundation  $\zeta_h$  that is a best match to the tsunami

MOM inundation  $\zeta_t$ . That is, we determine the hurricane category which satisfies

$$\min_c (|\zeta_{h_c} - \zeta_t|), \quad c = \text{Cat1}, \dots, \text{Cat5} \quad (1)$$

for each grid cell. The inundation level for the best-match category is denoted  $\zeta_{h_{\min}}$ . The actual difference between hurricane and tsunami inundation levels  $\Delta\zeta = \zeta_{h_{\min}} - \zeta_t$  then indicates how close of a match the best-match category actually is. Thus, positive values of  $\Delta\zeta$  indicate where hurricane storm surge inundation is higher than tsunami inundation, and negative values indicate where tsunami inundation is higher. A common local practice in tsunami modeling is to only consider inundation above a threshold of 0.3 m (1 ft) (Horrillo et al. 2011; Horrillo et al. 2015). This is due to the extensive flat and low-lying elevation found along the Gulf Coast. All depths are calculated for tsunami inundation modeling, but inundation less than 0.3 m (1 ft) is considered negligible here for inundation mapping purposes. Thus, comparisons are only made where either the tsunami or hurricane MOM inundation is at least 0.3 m (1 ft). Results for each of the five selected Gulf Coast communities are given in the following subsections.

**Fig. 18** Hurricane category which produces inundation at high tide that best matches the MOM tsunami inundation shown in Fig. 17 for the southern greater Tampa-St. Petersburg-Clearwater area. The contours drawn and labeled are at  $-5$  and  $-10$  m levels



### 3.1 South Padre Island, TX

South Padre Island, TX, is a barrier island in southern Texas located to the east of the mainland and Laguna Madre. Figure 2 shows the MOM tsunami inundation affecting South Padre Island. Note that inundation less than 0.3 m (1 ft) is not shown (same for all other figures of tsunami inundation). Clearly, the tsunami almost completely overtops the barrier island, as well as the northern part of the peninsula to the south. The highest inundation is seen at the beachfront, as could be expected, though significant inundation is seen across most of the island and peninsula past the dune system. Inundation also reaches across Laguna Madre to flood areas south of Port Isabel.

Figure 3 shows the hurricane category which best matches the tsunami inundation in South Padre Island. Figure 4 shows  $\Delta\zeta$  for the best-match hurricane category satisfying Eq. 1 and shown in Fig. 3. Note that pale colors (pale orange and yellow) in Fig. 4 and subsequent figures of  $\Delta\zeta$  indicate relatively good agreement between tsunami and storm surge inundation, i.e.,  $-0.5 \text{ m} \leq \Delta\zeta \leq 0.5 \text{ m}$  ( $-2 \text{ ft} \leq \Delta\zeta \leq 2 \text{ ft}$ ).

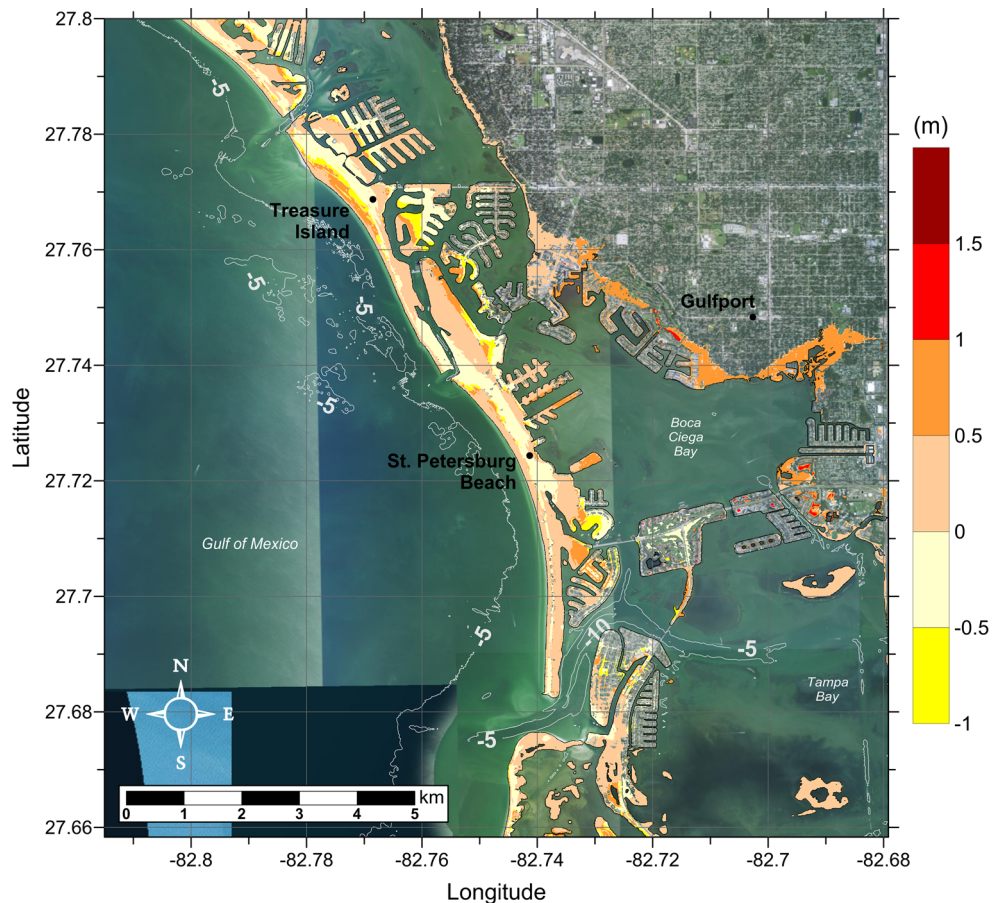
Clearly, the hurricane category best matching tsunami inundation in South Padre Island exhibits a decreasing trend

from the beach toward inland regions, as could be expected. Most of the barrier island experiences tsunami inundation comparable to a Category 3 or higher hurricane, with greater than Category 5 inundation seen at the immediate beachfront, significantly greater in some places (up to 5 m higher tsunami inundation than hurricane storm surge). Beyond the dune system, tsunami inundation is comparable to a Category 3-4, and at the lee part of the barrier island, tsunami inundation is on the order of a Category 3 hurricane. Across the channel/lagoon and into Port Isabel, tsunami inundation is on the order of a Category 1-2 hurricane.

### 3.2 Galveston, TX

Galveston, TX, is a barrier island situated to the south and southwest of Galveston Bay in coastal southeastern Texas. It is unique in that it features a protective seawall in front of the most populated portion of the island, built to protect the island from storm surge after the destructive Hurricane of 1900. Figure 5 shows the MOM tsunami inundation for the most populated part of Galveston, TX. For reference, the location of the seawall is indicated by a dashed black line (same for Figs. 6 and 7). Note that the domain shown here encompasses the entire section of the island that is protected

**Fig. 19** Actual difference  $\Delta\zeta$  (in meters) between SLOSH MOM storm surge inundation and maximum-of-maximums tsunami inundation for the best-match hurricane category shown in Fig. 18 for the southern greater Tampa-St. Petersburg-Clearwater area. Note that negative values indicate where tsunami inundation is higher than hurricane inundation, and pale colors indicate relatively good agreement between tsunami and storm surge inundation, i.e.,  $|\Delta\zeta| \leq 0.5 \text{ m}$ . The contours drawn and labeled are at  $-5$  and  $-10 \text{ m}$  levels



by the seawall. The island is fairly well protected from tsunami inundation due to the seawall bearing the brunt of the tsunami force, although the beach region just in front of the seawall as well as lower-lying areas at the east end of the island and to the southwest where water flows around the edge of the seawall experience higher inundation. Inundation also originates from the bay and channel at the lee part of the island, flooding portions of the island's northern side.

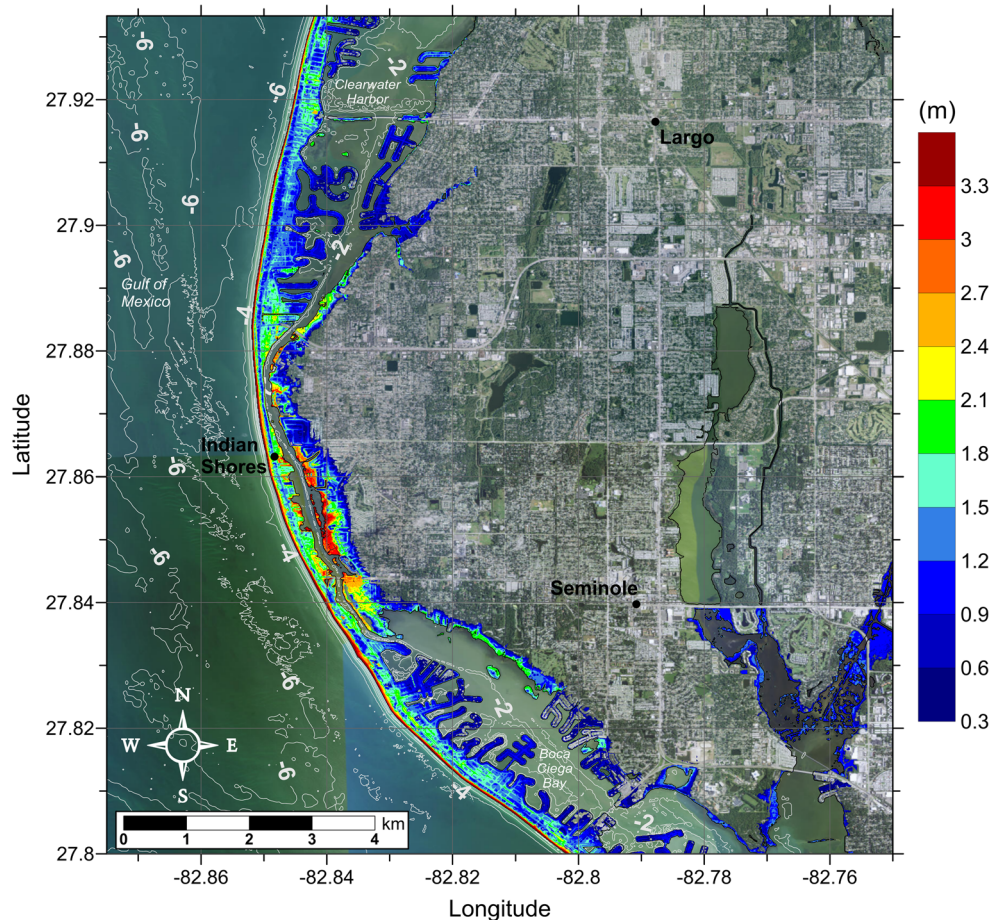
Figures 6 and 7 show the best-match hurricane category and  $\Delta\zeta$  for the best-match hurricane category, respectively, for Galveston. Tsunami inundation is comparable to a Category 1 or 2 hurricane throughout the majority of the flooded regions of the island with relatively good agreement ( $|\Delta\zeta| \leq 0.5$  m). Hurricane storm surge is slightly higher than tsunami inundation particularly toward the back part of the island where storm surge inundates from Galveston Bay and Offatts Bayou. Tsunami inundation on the order of a Category 3-4 hurricane is seen in low-lying areas in front of the seawall, with tsunami inundation slightly higher than that for storm surge in some isolated places mostly toward the west end of the island near the end of the seawall.

### 3.3 Mobile, AL

MOM tsunami inundation and comparisons with storm surge are performed for two specific areas of the greater Mobile, AL region: Dauphin Island/Gulf Highlands and the immediate Mobile area. Dauphin Island, a barrier island, and Gulf Highlands, which sits on a barrier peninsula, are both located at the mouth of Mobile Bay. Mobile, AL itself is situated at the northern edge of Mobile Bay.

Figure 8 shows tsunami inundation for Dauphin Island/Gulf Highlands. Clearly, these barrier regions are almost completely overtopped by the tsunami, with the highest inundation seen at the beachfront. Figure 9 shows the best-match hurricane category and Fig. 10 shows  $\Delta\zeta$  for the best-match hurricane category for this region. Crossing Dauphin Island and the peninsula of Gulf Highlands, there is a general decrease in the best-match hurricane category. Across the eastern part of Dauphin Island, tsunami inundation is comparable to a major hurricane: Category 4-5 hurricane at the beachfront and Category 3-4 at the eastern tip of the island. Category 1-2 levels are seen at the back-side of this portion of the island. The narrow western part of the island experiences tsunami inundation at Category

**Fig. 20** Maximum of maximums tsunami inundation depth (in meters) in the northern greater Tampa-St. Petersburg-Clearwater area, calculated as the maximum inundation depth in each grid cell from an ensemble of all tsunami sources considered. The contours drawn and labeled are at  $-2$ ,  $-4$ , and  $-6$  m levels



3-4 levels across its entire width. On the peninsula containing Gulf Highlands, tsunami inundation is greater than a Category 5 at the beachfront, significantly so (up to 5.5 m  $\approx$  18 ft higher) toward the east. Tsunami inundation is comparable to a Category 5 hurricane across much of the peninsula, decreasing to a Category 2-3 at the western half of the lee part of the peninsula, though Category 4 levels are still seen along the eastern half.

Tsunami inundation for the immediate Mobile, AL area is shown in Fig. 11. Mobile's position at the northern end of Mobile Bay largely protects it from tsunami inundation since most wave energy is dissipated across the barrier island/peninsula at the mouth of the bay. Only minor inundation is seen along the shores of the bay and inland waterways. Figures 12 and 13 show the best-match high tide hurricane category and  $\Delta\zeta$  for the best-match hurricane category, respectively, for Mobile. While Mobile is threatened by hurricane storm surge due to Mobile Bay and the numerous rivers and inland waterways being filled with water by consistent wind forcing during a storm event, its position at the north of Mobile Bay provides protection from significant tsunami inundation since most tsunami wave energy is expended as it crosses the barrier island region. As a result,

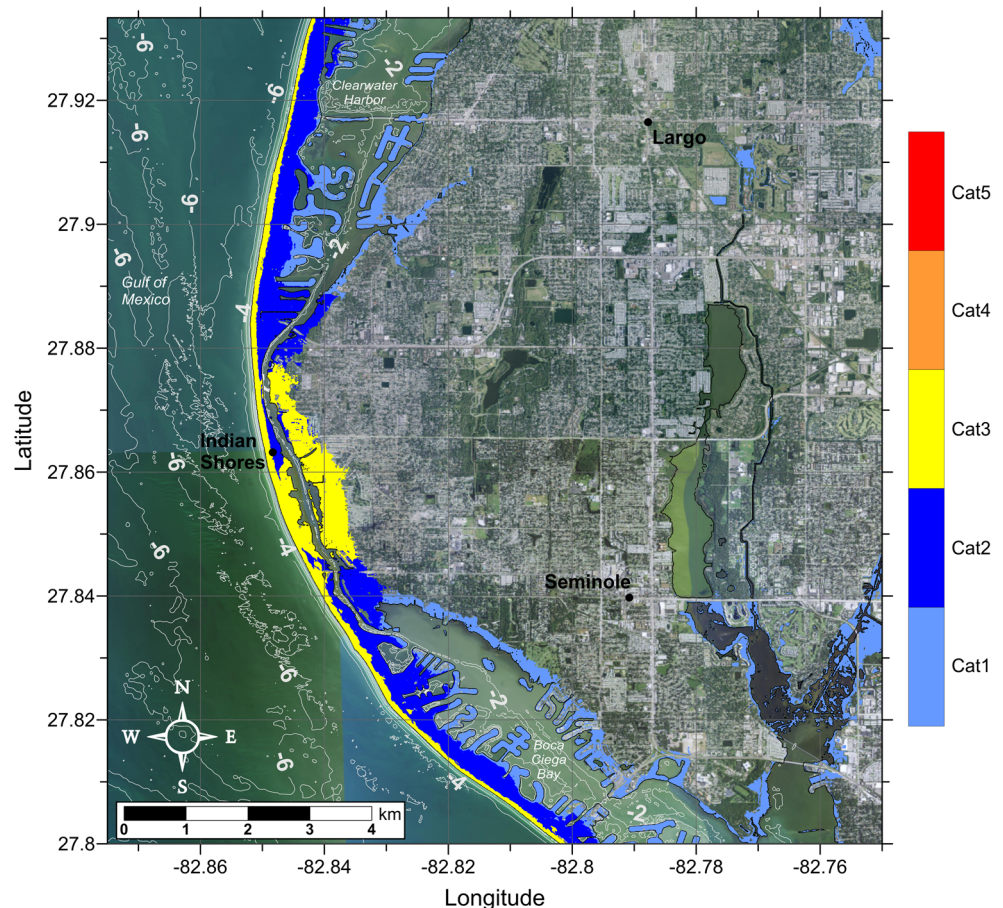
tsunami inundation is mostly less than that for a Category 1 hurricane in the immediate Mobile area.

### 3.4 Panama City, FL

Figure 14 shows MOM tsunami inundation for the greater Panama City, FL region, which includes barrier peninsulas connecting to the mainland surrounding St. Andrew Bay in the coastal panhandle of Florida. This region experiences widespread tsunami inundation with significant (greater than 6.3 m  $\approx$  21 ft) inundation depth at the beachfront and overtopping the dune system. Inundation depths of up to 1.5 m (5 ft) are seen reaching 5 km (3 mi) inland of the beachfront. This is most likely due to water traveling from low-lying areas northwest of Panama City Beach. Inundation also originates from inland waterways such as the Grand Lagoon.

Figure 15 shows the best-match hurricane category and Fig. 16 shows  $\Delta\zeta$  for the best-match hurricane category for Panama City. Overall, tsunami inundation is comparable to a major hurricane throughout most of this domain. Throughout most of the beachfront area and reaching well inland, tsunami inundation is significantly higher than that

**Fig. 21** Hurricane category which produces inundation at high tide that best matches the MOM tsunami inundation shown in Fig. 20 for the northern greater Tampa-St. Petersburg-Clearwater area. The contours drawn and labeled are at  $-2$ ,  $-4$ , and  $-6$  m levels



of a Category 5 hurricane (up to 8.5 m  $\approx$  28 ft higher than the storm surge inundation in some beach areas). Comparable hurricane category steadily decreases from Category 5 to Category 2 moving north starting approximately 4 km (2.5 mi) inland. Around the Grand Lagoon, tsunami inundation is on the order of a Category 3-5 hurricane, and across St. Andrew Bay along the mainland coast, tsunami inundation is comparable to Category 2-3 levels.

### 3.5 Tampa, FL

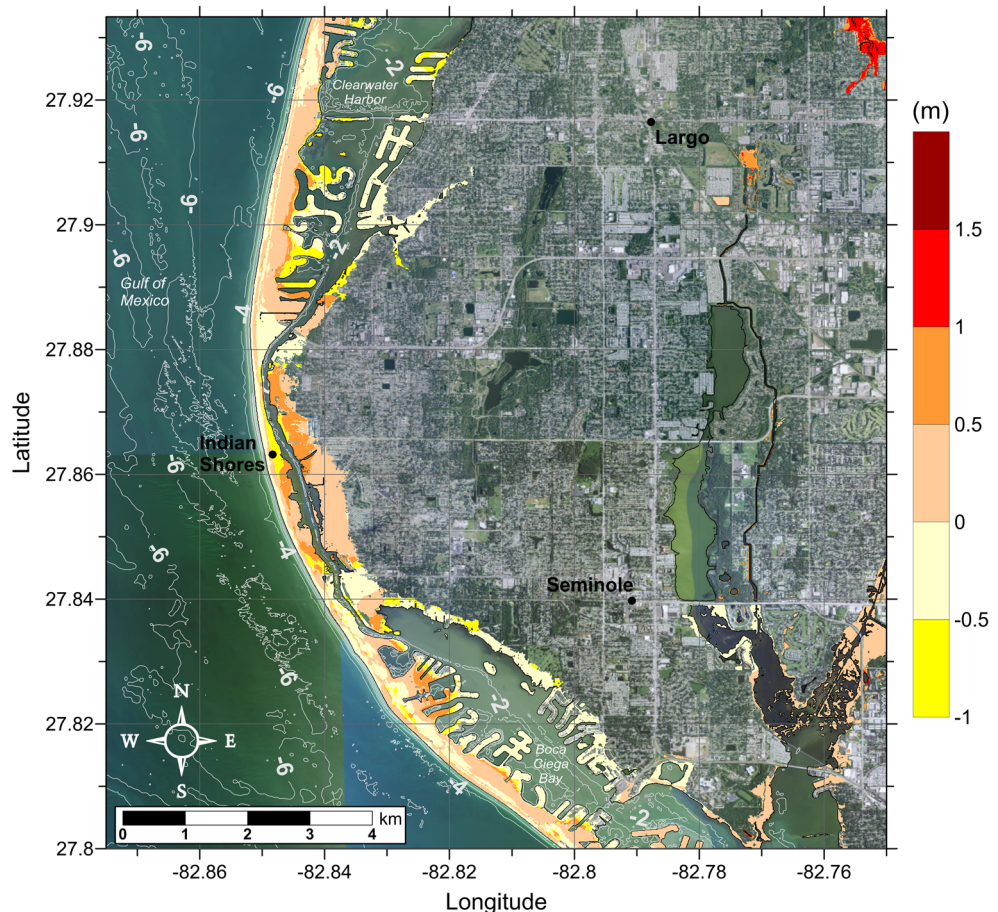
Comparisons of MOM tsunami inundation and storm surge are performed for the greater Tampa-St. Petersburg-Clearwater area, which includes a quite complex system of barrier islands and inlets along the western Florida peninsula and is separated here into a southern and northern region for visualization purposes.

Figure 17 shows the MOM tsunami inundation for the southern part of the greater Tampa-St. Petersburg-Clearwater area. The complexity of the barrier-inlet system provides many possible trajectories for tsunami waves to inundate the small residential islands in this community,

but also many obstacles to dissipate tsunami energy. As a result, inundation is seen mostly along the immediate beachfront and in some small islands forming the inland canals behind the main barrier island. Figures 18 and 19 show the best-match hurricane category and  $\Delta\zeta$ , respectively, for this region. In general, tsunami inundation is comparable to Category 3 levels at the beachfront decreasing to Category 1 at the lee part of the barrier islands and inland across the various bays and inlets.

Tsunami inundation for the northern part of the greater Tampa-St. Petersburg-Clearwater area is shown in Fig. 20. This region receives more inundation than the south particularly near where the mainland is in close proximity to the barrier island and thus the highest tsunami energy. Figures 21 and 22 show the best-match hurricane category and  $\Delta\zeta$ , respectively. As in the south, tsunami inundation is comparable to a Category 1-3 hurricane: Category 3 at the beachfront decreasing to Category 1 at the lee part of the barrier islands and into the mainland. The area around Indian Shores also experiences tsunami inundation on the order of a Category 3 hurricane reaching approximately 1 km (0.6 mi) inland on the mainland. This is most likely due

**Fig. 22** Actual difference  $\Delta\zeta$  (in meters) between SLOSH MOM storm surge inundation and maximum-of-maximums tsunami inundation for the best-match hurricane category shown in Fig. 21 for the northern greater Tampa-St. Petersburg-Clearwater area. Note that negative values indicate where tsunami inundation is higher than hurricane inundation, and pale colors indicate relatively good agreement between tsunami and storm surge inundation, i.e.,  $|\Delta\zeta| \leq 0.5$  m. The contours drawn and labeled are at  $-2$ ,  $-4$ , and  $-6$  m levels



to a focusing of tsunami energy at this location and the close proximity of the mainland to the barrier island.

#### 4 Conclusions

Tsunami inundation in five Gulf Coast communities was modeled considering seven submarine landslide tsunami sources spread across the northern GOM. Level and extent of maximum of maximums (MOM) tsunami inundation in each community varies depending on the regional variations in bathymetry/elevation. South Padre Island, TX, Dauphin Island/Gulf Highlands, AL, and Panama City, FL, receive the most inundation, in both depth and extent, overall. Panama City receives the most widespread inundation. Galveston, TX, is fairly well protected from inundation due to a seawall protecting the most populated part of the island. Most inundation in the greater Tampa-St. Petersburg-Clearwater area is seen to the north, while in the south, inundation occurs mostly along the immediate beachfront and in some small islands behind the main barrier island. Mobile, AL, itself is largely protected from tsunami inundation by its position at the northern end of Mobile Bay.

Comparisons of MOM tsunami inundation to the SLOSH MOM high tide storm surge inundation indicate that while the details of referencing tsunami inundation to hurricane storm surge is dependent on local topographic effects, general regional trends can be identified. Immediate beachfront areas are inundated at levels comparable to major hurricanes (Category 3 or higher) with some places experiencing tsunami inundation that is well above Category 5 levels (5 m  $\approx$  16.5 ft higher or more in some localized places). High tsunami inundation levels are particularly associated with barrier islands and locations where the continental shelf is relatively narrow, e.g., South Padre Island, TX, Dauphin Island/Gulf Highlands, AL, and Panama City, FL. Where the continental shelf is wide or where the community is located more inland (e.g., Galveston, TX, Mobile, AL, and the greater Tampa, FL area), tsunami inundation depths seem to be generally comparable to a Category 3 hurricane at the immediate beachfront with small stretches of Category 4 levels possible, and down to Category 1 levels in more inland areas. It is worth noting that for Galveston, also a barrier island, the long stretches of Category 4 inundation levels seen just in front of the seawall where the beach is narrow suggest that, if the seawall were not present, it is possible that the hurricane comparison would be similar to the other barrier islands of South Padre Island and Dauphin Island/Gulf Highlands. Indeed, as seen with the 2011 Tohoku tsunami, seawalls and other coastal hard structures may not be able to withstand the force of tsunami

impact, and the protection these structures provide is only effective if they survive the tsunami without being breached and/or damaged.

Overall, the trends seen among the communities in this study suggest that comparing tsunami and hurricane storm surge inundation is a reasonable first effort in order to provide low-resolution hazard zone information for Gulf Coast communities which do not currently have or warrant high-resolution tsunami inundation maps. While we acknowledge that storm surge characteristics and underlying physical processes (time scale, triggering mechanism, inundation process, etc.) are notably different from those of tsunamis, the trends seen between tsunami and storm surge inundation for the communities studied here seem to generally provide reasonable estimates of potential tsunami inundation in terms of hurricane category. The largest differences between the two types of inundation are seen along the beachfront and in some back bay areas due to the differing physics involved in these flooding processes. Tsunami waves hit a coastline on a relatively short time scale (on the order of hours) with a large forward momentum flux, causing the immediate coast to receive the bulk of the wave force and inundation. Waves can also travel up inland waterways and rivers that connect to the ocean, with energy quickly decreasing with increasing distance from the open coast. On the other hand, hurricane storm surge can affect coastal regions for hours to days, and surface winds force excess water to fill inland waterways like a bathtub, allowing flooding to occur from the backsides of islands and in areas surrounding the inland waterways as that "bathtub" overflows. Furthermore, the geomorphology of the coast and continental shelf have different impacts on tsunami and storm surge processes. The wide continental shelf (e.g., to the west of the Florida peninsula) serves to dissipate the energy of the long-wavelength tsunami waves, resulting in lower inundation and comparable hurricane categories (e.g., in the greater Tampa area). Conversely, the narrower continental shelf allows deep-water tsunami waves to reach the coast faster and with less energy dissipation, resulting in relatively high and widespread flooding (as seen for example in Panama City). In general, the opposite effects are seen with storm surge. Wide continental shelves with mild slopes serve to increase the storm surge impact since the constant force of wind shear continually pushes water higher onto the shallow shelf. On the other hand, narrow shelves with steeper slopes lessen storm surge. As a result of these different flooding mechanisms, open beaches and areas behind a narrow continental shelf require higher hurricane categories in order for the resulting storm surge to get even close to the level of tsunami inundation, while back bay areas experience less tsunami inundation and thus comparable storm surge levels are skewed toward lower hurricane categories.

Since even general, low-resolution inundation information is useful for hazard mitigation efforts, we believe that these results can be extended to provide a preliminary, first-order estimate of potential tsunami hazard zones for other Gulf Coast communities that is accessible and understandable to regional emergency managers and more appropriate for the low-lying Gulf Coast than methods such as the 10 m (33 ft) elevation contour line. We anticipate that communities which lack detailed tsunami inundation maps, but which have modeled hurricane storm surge information, would be able to use the results presented here to estimate their potential tsunami hazard level based on their regional topographical/bathymetric features. In particular, we expect the following general regional trends to be useful:

- Immediate beachfront areas are inundated at levels comparable to major hurricanes (Category 3 or higher), while more inland areas are inundated at Category 1-2 levels.
- Coastal regions near a relatively wide continental shelf experience tsunami inundation depths which are generally comparable to a Category 3 hurricane at the immediate beachfront, with some stretches of Category 4 levels possible.
- Barrier islands and coastal regions near a relatively narrow continental shelf experience tsunami inundation depths which can be well above Category 5 levels.

We stress, however, that such results should be used only in a broad, regional sense given the differences seen among and within communities based on local details of bathymetry, topography, and geographical location within the GOM basin. There is no guarantee that comparison results will be identical in areas with similar topography, and comparisons should only be made after understanding the limitations and simplifications of the methodology presented here. Improvements to the methodology would clearly improve the reliability of comparisons. For example, given the large difference in resolution of the SLOSH model data (1 km) and tsunami inundation data (1/3 arc-second  $\approx$  10 m), the comparison between the two datasets would be greatly improved with increased resolution of the SLOSH model runs, or alternate data on category-specific hurricane storm surge. Additionally, a more detailed comparison could also be accomplished by comparison with probabilistic storm surge parameters, e.g., the 100- or 500-year hurricane surge event, which may provide more/better information in areas where there are large differences between the modeled tsunami inundation and that of the best-match hurricane category. Successful implementation of this approach would certainly require the availability of probabilistic data for the locations of interest in order

to develop a generalized probabilistic tsunami-storm surge comparison.

**Acknowledgments** Funding for A. Pampell-Manis and J. Horrillo was provided by the National Tsunami Hazard Mitigation Program (NTHMP) under awards NA12NWS4670014, Construction of Five Additional Tsunami Inundation Maps for the Gulf of Mexico and NA13NWS4670018, A Probabilistic Methodology for Hazard Assessment Generated by Submarine Landslide in the Gulf of Mexico. Funding for all authors was also provided by the NTHMP under award NA14NWS4670049, Implementing NTHMP-MMS Strategic Plan in Tsunami Hazard Mitigation Products for the Gulf of Mexico. The authors also wish to thank Chayne Sparagowski and Amy Godsey for their direction on hurricane storm surge comparisons, and Craig Harter for his assistance with processing of data for comparisons.

## References

- Basco D, Klentzman C (2006) On the classification of coastal storms using principles of momentum conservation. In: Proc 31st Int Conf. on Coastal Eng. ASCE
- Dugan B, Stigall J (2010) Origin of overpressure and slope failure in the Ursa region, northern Gulf of Mexico. In: Mosher DC, Shipp RC, Moscardelli L, Chaytor JD, Baxter CDP, Lee HJ, Urgeles R, Submarine Mass Movements and Their Consequences. Springer, Netherlands, pp 167–178
- Dunbar PK, Weaver CS (2008) U.S. States and Territories national tsunami hazard assessment: historical record and sources for waves. U.S. Department of Commerce, National Oceanic and Atmospheric Administration, National Geophysical Data Center Tech. Rep. No. 3
- Grilli ST, Taylor ODS, Baxter CDP, Marezki S (2009) A probabilistic approach for determining submarine landslide tsunami hazard along the upper east coast of the United States. *Mar Geol* 264:74–97
- Harbitz CB, Løvnholt F, Bungum H (2014) Submarine landslide tsunamis: How extreme and how likely? *Nat Hazards* 72(3):1341–1374
- Hirt CW, Nichols BD (1981) Volume of fluid method for the dynamics of free boundaries. *J Comput Phys* 39:201–225
- Horrillo J (2006) Numerical method for tsunami calculations using full Navier-Stokes equations and the volume of fluid method. University of Alaska Fairbanks, PhD thesis
- Horrillo J, Wood A, Williams C, Parambath A, Kim GB (2011) Construction of tsunami inundation maps in the Gulf of Mexico. Tech. rep. Award Number: NA09NWS4670006 to the National Tsunami Hazard Mitigation Program (NTHMP), National Weather Service Program Office, NOAA, avail. from <http://www.tamug.edu/tsunami/NTHMP.html>
- Horrillo J, Wood A, Kim GB, Parambath A (2013) A simplified 3-D Navier-Stokes numerical model for landslide-tsunami: application to the Gulf of Mexico. *J Geophys Res Oceans* 118:6934–6950. doi:10.1002/2012JC008689
- Horrillo J, Pampell-Manis A, Sweetman B, Sparagowski C, Parambath L, Shigihara Y (2015) Construction of five additional tsunami inundation maps for the Gulf of Mexico and a probabilistic methodology for hazard assessment generated by submarine landslides in the Gulf of Mexico Tech. rep. Award Number: NA12NWS4670014 and NA13NWS4670018 to the National Tsunami Hazard Mitigation Program (NTHMP), National Weather Service Program Office, NOAA, avail. from <http://www.tamug.edu/tsunami/NTHMP.html>

- Irish JL, Resio DT (2010) A hydrodynamics-based surge scale for hurricanes. *Ocean Eng* 37:69–81
- Kantha L (2006) Time to replace the Saffir-Simpson hurricane scale? *Eos Trans AGU* 87(1):3–6
- Knight W (2006) Model predictions of Gulf and Southern Atlantic Coast tsunami impacts from a distribution of sources. *Sci Tsunami Haz* 24:304–312
- López-Venegas AM, Horrillo J, Pampell-Manis A, Huérfano V, Mercado A (2015) Advanced tsunami numerical simulations and energy considerations by use of 3D - 2D coupled models: The October 11, 1918, Mona Passage tsunami. *Pure Appl Geophys* 172(6):1679–1698
- Maretzki S, Grilli S, Baxter CDP (2007) Probabilistic SMF tsunami hazard assessment for the upper east coast of the United States. In: Lykousis V, Sakellariou D, Locat J, (eds) *Submarine Mass Movements and Their Consequences*. Springer, Netherlands, pp 377–385
- Masson D, Habitz C, Wynn R, Pederson G, Lovholt F (2006) Submarine landslides: processes, triggers and hazard protection. *Philos Trans R Soc A* 364:2009–2039
- Pampell-Manis A, Horrillo J, Shigihara Y, Parambath L (2016) Probabilistic assessment of landslide tsunami hazard for the northern Gulf of Mexico. *J Geophys Res Oceans*. doi:[10.1002/2015JC011261](https://doi.org/10.1002/2015JC011261)
- ten Brink US, Lee HJ, Geist EL, Twichell D (2009a) Assessment of tsunami hazard to the U.S. East Coast using relationships between submarine landslides and earthquakes. *Mar Geol* 264:65–73
- ten Brink US, Twichell D, Lynett P, Geist E, Chaytor J, Lee H, Buczkowski B, Flores C (2009b) Regional assessment of tsunami potential in the Gulf of Mexico. *U S Geol Surv Admin Rep*
- Yamazaki Y, Kowalik Z, Cheung KF (2008) Depth-integrated, non-hydrostatic model for wave breaking and run-up. *Int J Numer Methods Fluids* 61:473–497